

## Modelling measurement microphones using BEM with visco-thermal losses

Vicente Cutanda Henríquez and Peter M. Juhl

Institute of Technology and Innovation, University of Southern Denmark

Campusvej 55, 5230 Odense M, Denmark

vch@iti.sdu.dk, pmjuhl@iti.sdu.dk

For many decades, models that can explain the behaviour of measurement condenser microphones have been proposed in the literature. These devices have an apparently simple working principle, a charged capacitor whose charge varies when one of its electrodes, the diaphragm, moves as a result of sound waves. However, measurement microphones must be manufactured very carefully due to their sensitivity to small changes of their physical parameters. There are different elements in a microphone, the diaphragm, the gap behind it, a back cavity, a vent for pressure equalization and an external medium. All these subsystems form a strongly coupled device that cannot be modelled properly as a superposition of submodels, but rather as a whole. For this reason, the challenge of microphone modelling is still an ongoing area of research. In this work, a newly developed Boundary Element Method implementation that includes visco-thermal losses is used to model measurement condenser microphones. The models presented are fully coupled and include a FEM model of the diaphragm. The behaviour of the acoustic variables in the gap and the effect of the pressure equalization vent are discussed, as well as the practical difficulty due to the production variability among single units of the same microphone model.

### 1 Introduction

Measurement of sound pressure is mostly performed using microphones of the condenser type. There are many variations among these devices, but they all share common features. There is a conductive diaphragm, exposed to the sound waves on the one side, and closely backed by a conductive plate on the other side. The two elements form a capacitor that must be charged electrically to create a voltage. The variation of the capacitance due to the diaphragm movements induced by the sound field can then be sensed as voltage changes.<sup>1</sup>

Condenser microphones have a narrow space between the diaphragm and the back plate, usually only a few micrometers thick. This is desired for two reasons: i) the capacitance is larger the closer the electrodes, and ii) the film of air trapped in between can be adjusted to damp the diaphragm natural resonances by means of the viscous and thermal losses. The back plate distance and design can be chosen in order to fulfil these objectives and obtain the desired sensitivity, noise floor and bandwidth of the device. The back plate is in many cases provided with holes or slits and a connected back cavity in the interior of the microphone, all of them carefully balanced. Figure 1 shows a photograph and a sketch of a condenser microphone.

The acoustical and mechanical coupling of the external medium, the diaphragm, the narrow gap of air, the holes and the back cavity is indeed very strong and sensitive to parameters such as diaphragm tension and thickness of the air gap. Single units of the same measurement microphone model differ slightly in their performance and must be adjusted and calibrated individually.<sup>2</sup>

The design and analysis of condenser microphones is still mainly based on lumped parameter models.<sup>3</sup> For several decades, modelling of condenser microphones has been a recurring topic in the literature.<sup>4-9</sup> The proposed models combine analytical and lumped parameter representations of the elements of the device: external medium, diaphragm, thin air film, holes and back plate. Some authors introduce numerical models of some of these elements, but in most cases the visco-thermal effects in the thin air gap are represented by analytical formulas or lumped parameters. In

reference [9], the Finite Element Method is used when accounting for viscous and thermal losses; however, the comparison with measured results of the sensitivity and membrane displacement does not seem totally satisfying. The Finite Element Method (FEM) approach has demonstrated its validity for a simplified microphone geometry, the same used in the first example in this paper.<sup>10,11</sup>

Viscous and thermal losses are usually neglected when modeling sound waves, or rather accounted for as boundary impedance. This is due to the fact that most of the viscous and thermal effects occur within a thin layer over the boundary, with a thickness of a fraction of a millimeter to a few micrometers depending on the frequency. However, setups where the dimensions are small enough to be of the same range as the visco-thermal boundary layer need more advanced models that include losses. To do so, a linearized version of the Navier-Stokes equations for fluids must be used, either directly in a FEM implementation or through the Kirchhoff decomposition of these equations into acoustic, thermal and viscous components.<sup>12,13</sup> In this paper the Kirchhoff decomposition in combination with the Boundary Element Method (BEM) is used.<sup>14-18</sup>

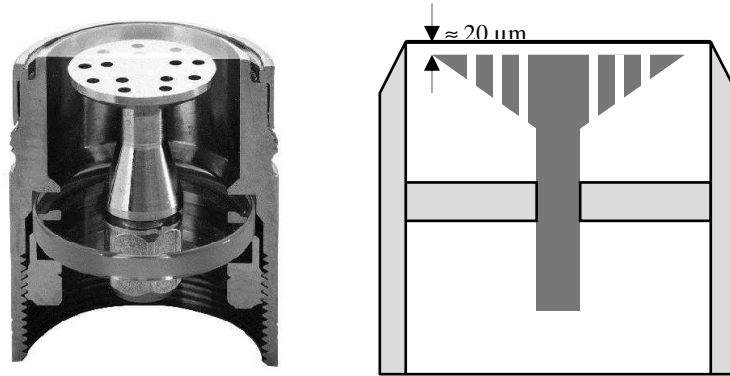


Figure 1. Photograph (source: Brüel & Kjær) and diagram of a condenser microphone, showing its interior.

The paper will present the adaptation of a custom-made implementation of the Boundary Element Method, the OpemBEM, to include viscous and thermal losses. An axisymmetrical implementation is chosen which is convenient for the geometry of condenser microphones. Two calculation examples are calculated: i) an idealized geometry with no back cavity, and ii) a Brüel & Kjær measurement microphone with a back cavity and no holes in the back plate. The results are compared with an analytical model and electrostatic actuator measurements respectively.

## 2 Visco-thermal equations

Sound propagation in a fluid with losses can be described using three decoupled modes: i) an acoustic mode describing the part of the wave that propagates, ii) a thermal mode, which includes the effect of thermal losses and iii) a viscous mode, with the losses by viscous friction.<sup>12-14</sup> The harmonic equations representing the three effects are:

$$\begin{aligned} (\Delta + k_a^2) p_a &= 0 \\ (\Delta + k_h^2) p_h &= 0 \\ (\Delta + k_v^2) \vec{v}_v &= \vec{0} \quad \text{with} \quad \nabla \cdot \vec{v}_v = 0 \end{aligned} \tag{1,2,3}$$

where the indexes  $a$ ,  $h$  and  $v$  indicate respectively acoustic, thermal and viscous modes and the total pressure is  $p = p_a + p_h$ , since the viscous velocity has no pressure associated. The wavenumbers  $k_a$ ,  $k_h$  and  $k_v$  are a function of the perfect fluid wavenumber  $k$  and several physical parameters, such as viscosity, bulk viscosity, thermal conductivity, etc. The harmonic time dependence  $e^{i\omega t}$  is omitted.

Equations (1), (2) and (3) and the modes they represent are decoupled in the fluid, but they are linked through the boundary conditions. The viscous and thermal modes are particularly strong within a thin boundary layer on the boundary surface, caused respectively by the no-slip condition of the tangential velocity and the thermal absorption of the surface. The viscous and thermal boundary layers have a thickness that is inversely proportional to the square root of the frequency, and at audio frequencies it spans from a fraction of a millimeter to a few micrometers.

The boundary condition for the pressure is a consequence of the high thermal conductivity the boundary, creating isothermal conditions. Since the pressure is related to the temperature, it must be:

$$\bar{T} = T_a + T_h = \tau_a p_a + \tau_h p_h = 0 \quad (4)$$

The parameters  $\tau_a$  and  $\tau_h$  depend on the physical properties of the fluid and the frequency.

The velocity boundary condition, in opposition to the classical normal velocity condition for perfect fluids, has a vectorial nature for fluids with losses. This means that the total velocity vector, the sum of all three modes, must match the movement of the boundary in the normal (noted  $n$ ) and tangential (noted  $t$ ) directions, that is,

$$\bar{v}_{boundary} = \bar{v}_a + \bar{v}_h + \bar{v}_v.$$

If the thermal and acoustic velocities are expressed as a function of the corresponding pressures:

$$\bar{v}_{boundary} = \phi_a \nabla p_a + \phi_h \nabla p_h + \bar{v}_v \quad (5)$$

where  $\phi_a$  and  $\phi_h$  depend on physical constants and the frequency. This vectorial condition is split into normal and tangential components, the latter being a two-dimensional vector expression:

$$v_{boundary,n} = \phi_a \frac{\partial p_a}{\partial n} + \phi_h \frac{\partial p_h}{\partial n} + v_{v,n} \quad (6)$$

$$\bar{v}_{boundary,t} = \phi_a \nabla_t p_a + \phi_h \nabla_t p_h + \bar{v}_{v,t} \quad (7)$$

Equation (7) is the so-called no-slip condition because the fluid must follow the tangential movement of the setup at the boundary.

### 3 The Boundary Element Method with visco-thermal losses.

#### 3.1 Axisymmetrical BEM

Equations (1) to (3) are all of the Helmholtz type (note that Eq. (3) is vectorial and in reality represent three equations – one for each component) and therefore well suited for the Boundary Element Method. However, the numerical implementation has certain differences when compared to implementations of the standard (lossless) Helmholtz equation, since the wavenumbers  $k_h$  and  $k_v$  have large imaginary values and represent fast decaying fields, which must be carefully handled in the numerical integration.

It is beyond the scope of the present paper to give a detailed account of the mathematical manipulations, but using the boundary conditions (Eq's (4), (6) and (7)) allows for the elimination of variables and results in an expression relating the acoustic pressure  $p_a$  to the normal component of the boundary velocity  $v_{boundary,n}$  assuming that the tangential boundary velocity is zero:

$$\mathbf{v}_{boundary,n} = \mathbf{VT} \mathbf{p}_a \quad (8)$$

where the matrix  $\mathbf{VT}$  is a combination of matrices resulting from the discretized versions of Eq.'s (1) to (3) linked through the boundary conditions

In this paper an axisymmetrical formulation of the BEM is used, which has been programmed in the OpenBEM Matlab code. The objects to be modeled must have axial symmetry, and only their generator needs to be meshed.

### 4 Model of an idealized microphone

A simple geometry of a microphone with an analytical solution can be found in reference [11]. This example has been used previously in the literature for comparison with numerical models.<sup>10,14</sup> The microphone is a circular diaphragm stretched over a circular cavity and a hard back plate, forming a flat cylinder. The rim of the structure is set with a pressure release boundary condition ( $p=0$ ) and excited by a uniform sound pressure on the membrane. The setup is sketched in figure 2. The surfaces of diaphragm and back plate are close enough to cause problems in a standard BEM formulation; this difficulty has been dealt with using an improved integration strategy.<sup>19</sup>

In principle, the boundary surface must be differentiable at least once (no sharp corners) in order for the surface derivatives to exist.<sup>13</sup> Sharp corners are nevertheless implemented in order to observe the effect on the solution.

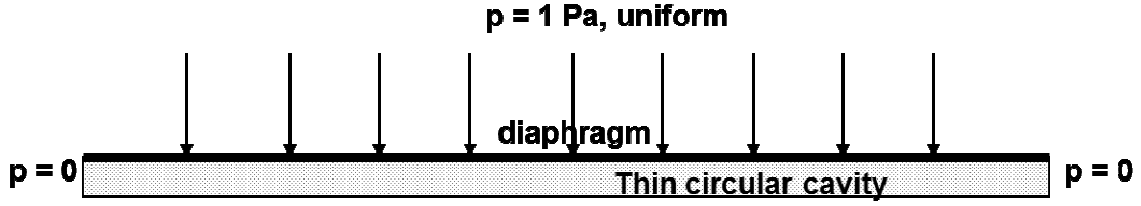


Figure 2. Sketch of the idealized microphone in reference [11].

The radius of the microphone is 2 mm and the gap thickness is 18  $\mu\text{m}$ . The diaphragm tension is 3128 N/m, the density of the diaphragm material is 8300  $\text{kg/m}^3$  and the diaphragm thickness is 6,95  $\mu\text{m}$ .

#### 4.1 Model of the diaphragm

The diaphragm is modelled as a membrane with no stiffness, following the equation:

$$\frac{\partial^2 \varepsilon}{\partial r^2} + \frac{1}{r} \frac{\partial \varepsilon}{\partial r} + K^2 \varepsilon = \frac{p_d}{T} \quad (9)$$

where  $\varepsilon$  is the normal displacement,  $K$  is the wavenumber of the mechanical wave,  $T$  is the membrane tension and  $p_d$  is the sum of sound pressures acting on the diaphragm, internal and external.<sup>4,5</sup> This equation is implemented using a one-dimensional Finite Element Method implementation producing the matrix equation:

$$(\mathbf{A}_m + K^2 \mathbf{B}_m) \boldsymbol{\varepsilon} = \frac{P_d}{T} \quad (10)$$

#### 4.2 Coupled model of the idealized microphone

The coupled system of equations for the idealized microphone is:

$$\begin{pmatrix} T(\mathbf{A} + K^2 \mathbf{B}) & \mathbf{D} \\ -i\omega & \mathbf{VT} \end{pmatrix} \begin{pmatrix} \vdots \\ \varepsilon_i \\ \vdots \\ \vdots \\ p_a \\ \vdots \end{pmatrix} = \begin{pmatrix} \vdots \\ p_{inc} \\ \vdots \\ \vdots \\ 0 \\ \vdots \end{pmatrix} \quad (11)$$

where equation (10) can be seen in the top rows of the system of equations. The term  $\mathbf{VT}$  represents equation (8) and  $\mathbf{D}$  and  $-i\omega$  are coupling matrices:  $\mathbf{D}$  represents forces on the diaphragm from the acoustic pressure and  $-i\omega$  represents the membrane movement as a boundary velocity for the acoustic part. The  $p_a$  are the pressures on the nodes in the interior of the microphone,  $p_{inc}$  are the contributions of the external pressure on the diaphragm nodes, and the  $\varepsilon_i$  are the displacements of the diaphragm nodes.

#### 4.3 Results

The sensitivity of the idealized microphone is calculated by integrating the diaphragm displacement over the area of the diaphragm which is proportional to the sensitivity of the microphone<sup>14,17</sup>.

The sensitivity shown in figure 3 has been calculated for a range of meshes with varying number of elements and allowing in some cases sharp corners on the rim. The calculation does not break down when the mesh density is reduced or the corners are made sharp, and the agreement for the rougher meshes can be acceptable for initial calculations. The effect of rounding the corners is less evident the more elements in the mesh. The finer mesh, with 176 elements, is almost identical to the analytical solution. All curves, analytical and numerical, are normalized with the same value.

Both analytical and numerical solutions are able of producing results of the viscous, thermal and acoustic magnitudes independently, both on the boundary and in the microphone's interior. As an example, the radial component of the particle velocity is shown in figure 4 for several frequencies along a line in the  $z$  direction and at a distance midway

from the centre to the rim. The boundary layer can be seen clearly: the fluid is forced to be still by the diaphragm and back plate surfaces.

Figure 5 shows membrane displacement for the same frequencies and along a radius. The match with the analytical solution is quite good in all cases, so much that the curves are almost identical.

The results shown in figures 3, 4 and 5 were calculated with one of the finer meshes, with 176 elements. The values shown in figure 4 are calculated in the domain, that is, the BEM results on the surface are used in an additional calculation where domain points are obtained. The process is not direct in the case of the viscous component of the particle velocity, since the surface results are given in a boundary reference system (tangential and normal components), which needs to be transported to the global coordinate system. On the other hand, the thermal and acoustic components of the particle velocity are calculated as finite difference gradients of the domain pressures. The outcome is however satisfactory.

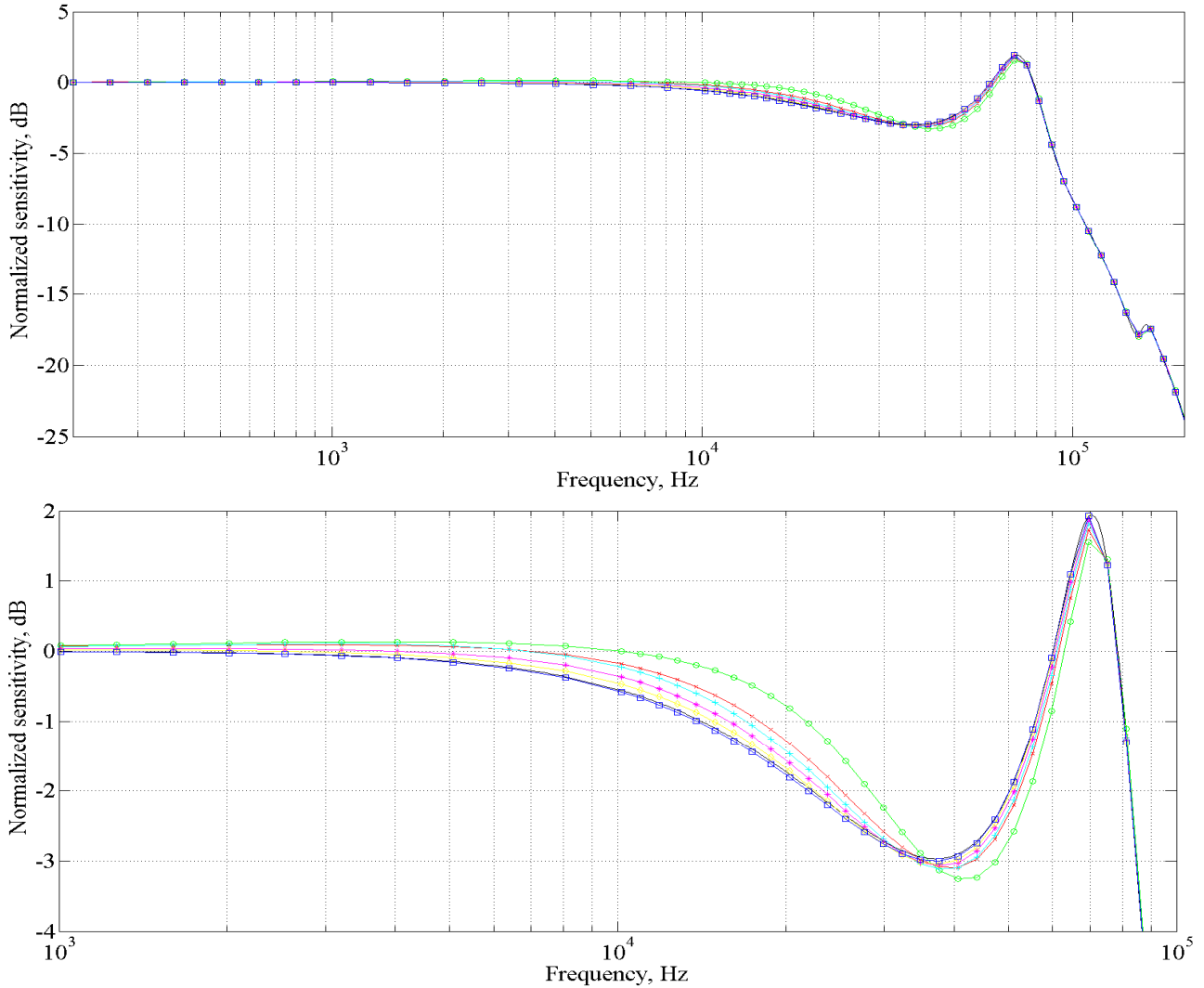


Figure 3. Normalized sensitivity of the idealized microphone. The lower plot is a zoomed-in version of the upper one. Continuous black line, analytical solution; “x”, 31 elements, rounded corners; “o”, 25 elements, sharp corners; “+”, 45 elements, sharp corners; “\*”, 51 elements, rounded corners; “◇”, 100 elements, rounded corners; “□”, 176 elements, rounded corners.

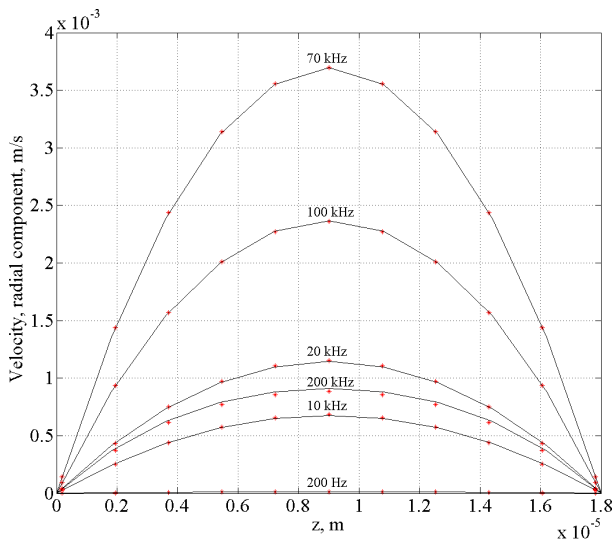


Figure 4. Radial component of the particle velocity along a vertical line traversing the gap halfway from the centre to the rim. ‘\*’, BEM calculation; continuous line, analytical solution.

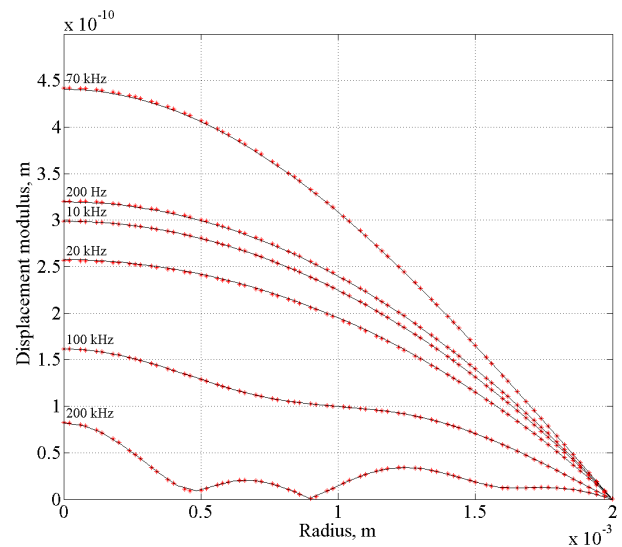


Figure 5. Membrane displacement, over a radial direction. ‘\*’, BEM calculation; continuous line, analytical solution.

## 5 Model of a measurement condenser microphone

The second example is a commercial measurement condenser microphone, where the coupled model calculations are compared with measurement results. The measured sensitivity frequency response is taken from the literature and is an electrostatic actuator measurement<sup>14</sup>. The chosen microphone is the Brüel & Kjær microphone type 4938, a ¼” pressure-field microphone with no holes in the back plate.<sup>20</sup> The microphone is therefore axisymmetrical and is suitable for modelling using the axisymmetrical BEM. The only non-axisymmetrical feature is the pressure equalization vent on the side, which is modelled as a pressure-release circular slit. The nominal parameters of the 4938 are listed in Table 1. However, during production, the microphone is individually adjusted in order to meet the model specifications. As a result, the microphone parameters and in particular the gap width and diaphragm tension vary from unit to unit and must be adjusted in the numerical model.

Figure 6 shows a picture of the 4938 and examples of BEM meshes employed to model the microphone’s internal and external boundaries. Note the different scales of the sub figures.

Table 1. Design parameters of the Brüel & Kjær microphone type 4938.

<b>Membrane radius (mm)</b>	2
<b>Backplate radius (mm)</b>	1,75
<b>Gap thickness (µm)</b>	18
<b>Membrane tension (N/m)</b>	3128
<b>Membrane density (kg/m<sup>3</sup>)</b>	8300
<b>Membrane thickness (µm)</b>	6,95

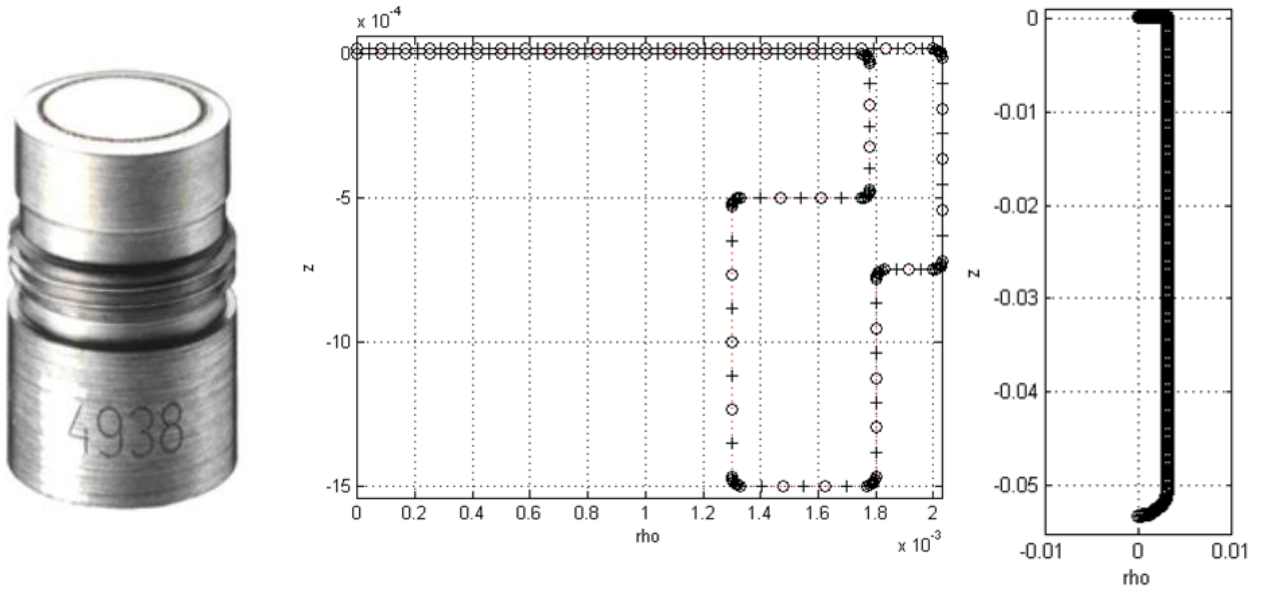


Figure 6. From left to right, a picture of the type 4938 microphone and examples of BEM generator's meshes of the interior and exterior domains.

## 5.1 Coupled model of the idealized microphone

The coupled system of equations for the BK4938 microphone is as follows:

$$\begin{pmatrix} T(\mathbf{A} + K^2\mathbf{B}) & \mathbf{D} & \mathbf{E} \\ -i\omega & \mathbf{VT} & \mathbf{0} \\ -i\omega & \mathbf{0} & \mathbf{B}_{ext}^{-1}\mathbf{A}_{ext} \end{pmatrix} \begin{pmatrix} \vdots \\ \varepsilon_i \\ \vdots \\ \vdots \\ p_a \\ \vdots \\ \vdots \\ p_e \\ \vdots \end{pmatrix} = \begin{pmatrix} \vdots \\ \mathbf{0} \\ \vdots \\ \vdots \\ \mathbf{0} \\ \vdots \\ \vdots \\ p_{inc} \\ \vdots \end{pmatrix} \quad (12)$$

Equation (12) includes the same terms as equation (11), with the additional coupling of the external domain, represented by the BEM coefficient matrices  $\mathbf{A}_{ext}$  and  $\mathbf{B}_{ext}$ . The term  $\mathbf{VT}$  represents equation (8), the term  $T(\mathbf{A} + K^2\mathbf{B})$  is equation (10), and  $\mathbf{D}$ ,  $\mathbf{E}$  and  $-i\omega$  are coupling matrices. The  $p_a$  are the pressures on the nodes in the interior of the microphone, the  $p_e$  are the scattering pressures on the external surface of the microphone and  $p_{inc}$  are the contributions of the external incident sound field on the external surface.

All the essential elements that play a role in the performance of the microphone are represented in this coupled system, with the exception of the electrostatic force. This force is not very relevant for this microphone type according to personal communication with Brüel & Kjær, and the results in this paper seem to support the idea. Electrostatic forces can easily be added as an excitation to the diaphragm nodes without extending the system of equations.

## 5.2 Results

Figure 7 compares the measured responses and the corresponding adjusted models. In figure 7, the model parameters are : gap thickness of 19,65  $\mu\text{m}$  (+9%), diaphragm tension of 3566 N/m (+14%), and diaphragm surface density of 61,1  $\text{g/m}^2$  (+6%). Numbers in parentheses are relative deviations from the nominal values

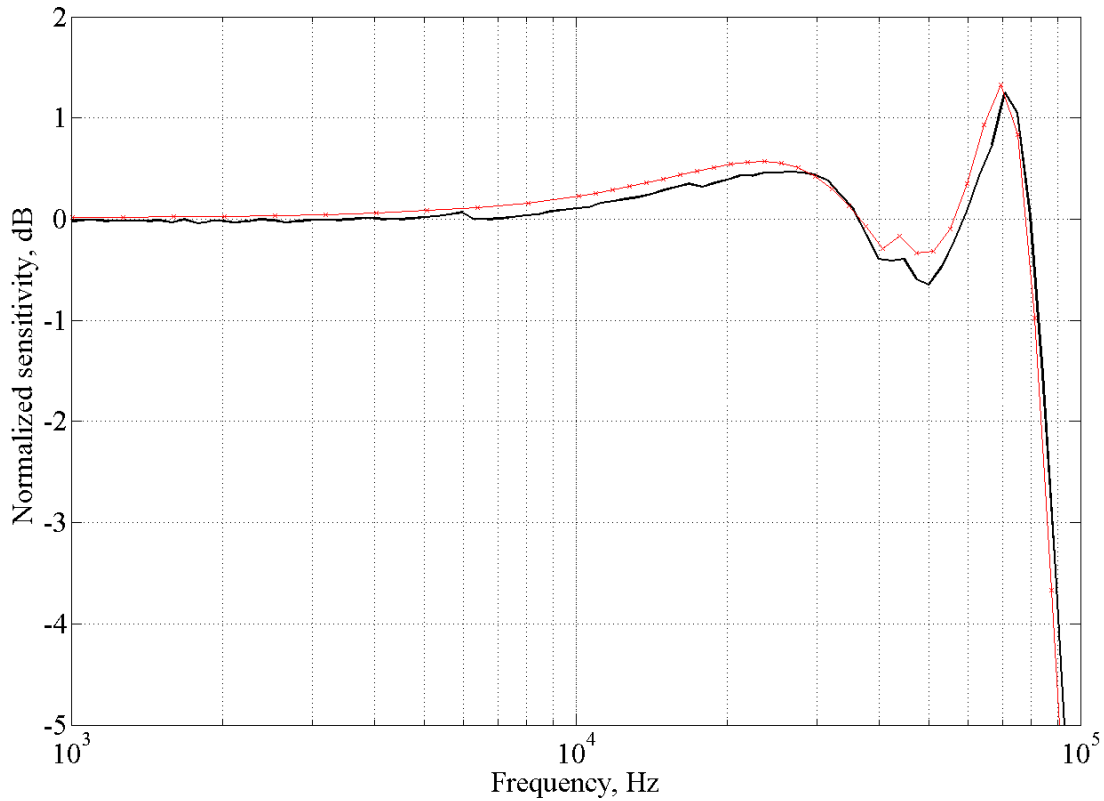


Figure 7. Sensitivity response: comparison between the actuator measurement in reference [14] and the adjusted numerical model. 'x', BEM calculation, continuous line, actuator response.

## 6 Conclusions

The main purpose of this paper, the modelling of the measurement condenser microphone, is achieved by means of a novel axisymmetrical BEM formulation with losses of the interior of the device that is included in a coupled model. The condenser microphone poses a particularly challenging modelling task, and it acts therefore as a test for the new BEM implementation.

Besides the inherent complicated nature of condenser microphones, their modelling is made yet more difficult because they are adjusted one by one during production in a way that prevents a sufficiently precise knowledge of their key parameters. Both measurements and simulations demonstrate that quite small changes in the construction parameters of the microphone can give rise to significant changes in its performance. The simulations of a theoretical microphone in section 4 demonstrate that the numerical model is able of coping with the task. When a real microphone is simulated in section 5, however, a parameter adjustment process is necessary in order to get a close model, and even then it is not possible to assume that the chosen set of parameters reflects reality. This is due to the microphone complexity, not a result of any modelling difficulty. Even in the case of the real microphone in section 5 and the fitting procedure, the sensitivity obtained differs only by a fraction of 1 dB.

The proposed model can nevertheless be used for studying the physical behaviour of the microphone, improve its design and adapt it to the systems where it is included. Primary and secondary calibration systems, couplers, hearing aids and mobile devices can benefit from an improved microphone model.

As to the BEM model with losses, it has shown its adequacy for this challenging modelling task with meshes that have fewer degrees of freedom than the corresponding FEM models in the literature. The model is robust enough to cope with sharp edges and corners, which in principle should be rounded for a precise representation.

The use of the Kirchhoff decoupling of viscous, thermal and acoustic modes combines well with the Boundary Element Method, since all the coupling is performed at the boundary, where the BEM boundary conditions are applied. If the coefficients of the BEM matrices are calculated properly, calculation in the domain follows easily.



## 7 Acknowledgement

The authors wish to thank Erling Sandermann Olsen and Johan Gramtorp from Brüel & Kjær, for their interest and support in this project.

## References

- [1] L. L. Beranek, *Acoustics*. Acoustical Society of America, New York, 1996.
- [2] *Brüel & Kjær Microphone Handbook*. Brüel & Kjær Sound & Vibration Measurement A/S, Nærum, Denmark, 1996.
- [3] F. V. Hunt, *Electroacoustics. The Analysis of Transduction, the analysis of transduction and Its Historical Background*. Acoustical Society of America, New York, 1982.
- [4] D. H. Robey, Theory of the Effect of a Thin Air Film on the Vibrations of a Stretched Circular Membrane. *Journal of the Acoustical Society of America*, 26(5), 740-745, 1954.
- [5] A. J. Zuckerwar, Theoretical response of condenser microphones. *Journal of the Acoustical Society of America*, 64(5), 1278-1285, 1978.
- [6] X. Bao and Y. Kagawa, A Simulation of Condenser Microphones in Free Field by Boundary Element Approach. *Journal of Sound and Vibration* 119(2), 327-337, 1987.
- [7] R. S. Grinnip III, Advanced Simulation of a Condenser Microphone Capsule. *J. Audio Eng. Soc.*, Vol. 54, No. 3, 2006.
- [8] Thomas Lavergne, Stéphane Durand, Michel Bruneau, and Nicolas Joly, Dynamic behavior of the circular membrane of an electrostatic microphone: Effect of holes in the backing electrode. *Journal of the Acoustical Society of America* 128 (6), 3459–3477, 2010.
- [9] D. Homentcovschi and R. N. Miles, An analytical-numerical method for determining the mechanical response of a condenser microphone, *Journal of the Acoustical Society of America* 130 (6), 3698–3705, 2011.
- [10] W. R. Kampinga, Y. H. Wijnant and A. de Boer, An Efficient Finite Element Model for Viscothermal Acoustics, *Acta Acustica united with Acustica*, 97, 618–631, 2011.
- [11] G. Plantier and M. Bruneau, Heat conduction effects on the acoustic response of a membrane separated by a very thin air film from a backing electrode. *Acoustique* 3, 243-250, 1990.
- [12] A. D. Pierce, *Acoustics. An Introduction to Its Physical Principles and Applications*. Acoustical Society of America, New York, 1989.
- [13] M. Bruneau, Ph. Herzog, J. Kergomard and J. D. Polack: General formulation of the dispersion equation in bounded visco-thermal fluid, and application to some simple geometries. *Wave Motion North Holland* 11, 441-451, 1989
- [14] V. Cutanda Henríquez, *Numerical transducer modeling*. PhD thesis, Technical University of Denmark, Lyngby, Denmark, 2002.
- [15] V. Cutanda Henriquez, P. M. Juhl : OpenBEM - An open source Boundary Element Method software in Acoustics. *Proceedings of Internoise 2010*. October 2010, Lisbon.
- [16] Vicente Cutanda Henríquez and Peter Møller Juhl, An Axisymmetrical Acoustic BEM Formulation Including Visco-Thermal Losses. *Proceedings of Forum Acusticum 2011*, Aalborg, Denmark, 2011.
- [17] P. M. Juhl, *The Boundary Element Method for Sound Field Calculations*. PhD Thesis. Technical University of Denmark, Lyngby, Denmark, 1993.
- [18] P.M. Juhl, An axisymmetric integral equation formulation for free space non-axisymmetric radiation and scattering of a known incident wave. *Journal of Sound and Vibration* 163 (1993), 397-406.
- [19] V. Cutanda Henríquez, P. M. Juhl and F. Jacobsen: On the Modeling of Narrow Gaps Using the Standard Boundary Element Method. *Journal of the Acoustical Society of America*, 109, 1296-1303 (2001).
- [20] *Brüel & Kjær Product Data Sheet BPI844, 1/4" Pressure-field Microphone – Type 4938*. Brüel & Kjær Sound and Vibration Measurement A/S, Nærum, Denmark, 2008.